On Symmetry Properties of Intrinsic Interference in FBMC-OQAM Systems

Vibhutesh Kumar Singh, Mark F. Flanagan and Barry Cardiff
School of Electrical and Electronic Engineering
University College Dublin, Belfield, Dublin 4, Ireland
Email: vibhutesh.k.singh@ieee.org, mark.flanagan@ieee.org, barry.cardiff@ucd.ie

***Abstract*—Filter bank multicarrier with offset quadrature amplitude modulation (FBMC-OQAM) is a modulation technique which is widely considered as a strong contender to replace cyclic prefixed orthogonal frequency division multiplexing (CP-OFDM), for the future 5th generation (5G) of mobile wireless communication networks. FBMC-OQAM exhibits good spectral confinement properties, high spectral efficiency and immunity to synchronization errors, mainly due to its prototype filter's localization properties. But these desirable traits come with the loss of orthogonality, rendering it only orthogonal for real symbols with imaginary interference appearing in both the frequency and time domains. In this work, we prove a set of symmetry properties of this interference for a general class of FMBC-OQAM systems, and use these relationships to derive autocorrelation matrices for interference from neighboring symbols and also for noise contributions. These matrices find application in receiver design and also in channel estimation. The derived symmetry properties are also demonstrated through numerical examples for various standard prototype filter designs.**

I. Introduction

Current broadband services are based on CP-OFDM or its variants. The advantages offered by this modulation scheme include low complexity implementation, robustness against multipath fading environment, orthogonality between sub-carriers, trivial implementation of the channel estimator and equalizer, and easy adaptation to the multiple-input multiple-output (MIMO) context [1]. However, many of these benefits come at the cost of reduced spectral efficiency through the use of the cyclic prefix, and high spectral leakage due to rectangular pulse shaping which leads to a sinc pulse shaped frequency spectrum. Therefore, research is underway targeting the design of an alternate future 5G waveform which will address all these concerns [2].

To overcome these issues, filter bank multicarrier (FBMC) is an attractive alternative to OFDM [3] which comes at the cost of higher computational complexity. Instead of the rectangular pulse shaping filter used for OFDM, the use of a smoothed pulse shape (typically based on a prototype filter) leads to reduced out of band emissions (OOBE). However, this new filter bank arrangement no longer produces a parallel bank of orthogonal sub-carriers; rather, they interfere with each other.

This publication has emanated from research supported by a research grant from Science Foundation Ireland (SFI) and is co-funded under the European Regional Development Fund under Grant Number 13/RC/2077.

978-1-5386-6046-1/18/$31.00 ©2018 European Union

The solution employed in FBMC-OQAM is to stagger, by half a symbol interval, the modulation of real-valued data symbols onto the in-phase and quadrature component of each sub-carrier. Then, by judicious pulse shaping filter design, it is arranged for the interference appearing on the outputs from a bank of matched filters in a receiver to be purely imaginary, thereby preserving orthogonality between the real valued symbols on each of the quadrature components. As this orthogonality is achieved without the need for a cyclic prefix (CP), the use of FMBC-OQAM not only offers improved OOBE but is also a more spectrally efficient modulation alternative to CP-OFDM. Some well-known prototype filter designs include PHYDYAS [4], Hermite [5], root raised cosine (RRC) [6] and half cosine [7].

While in principle the nature of the purely imaginary interference has little bearing on the symbol detection process, it does play an important role in channel estimation and also contributes to errors in receivers with imperfect channel state information (CSI). For this reason, several authors (e.g., [8], [9]) have computed these interference terms and derived relationships between them at immediate neighboring FT points for various prototype filter designs. In this paper, we prove five general symmetry laws obeyed by all prototype filters. We then use these symmetry results to derive in very general forms, the autocorrelation matrices of the interference and noise terms which affect the output of the bank of matched filters at the receiver. These results have immediate application in channel estimation.

This paper is structured as follows. Section II describes the system model, and the fundamental symmetry properties of the interference terms are derived in Section III. Application of these symmetry relationships to the computation of the interference and noise autocorrelation matrices is examined in Section IV. Finally, numerical results for well-known prototype filters are given in Section V, and Section VI presents conclusions.

Notations: Vectors and matrices are denoted by bold letters. For a matrix $\mathbf{A}$, $[\mathbf{A}]_{i,j}$ denotes its (i,j) entry. Superscripts T and $\mathcal{H}$ denote transpose and conjugate transpose of matrices respectively. $\Re(x)$ denotes the real part of a complex number x, while x^* denotes its complex conjugate. $\mathbb{Z}$ denotes the set of integers, E denotes the expectation operator, and $j = \sqrt{-1}$.

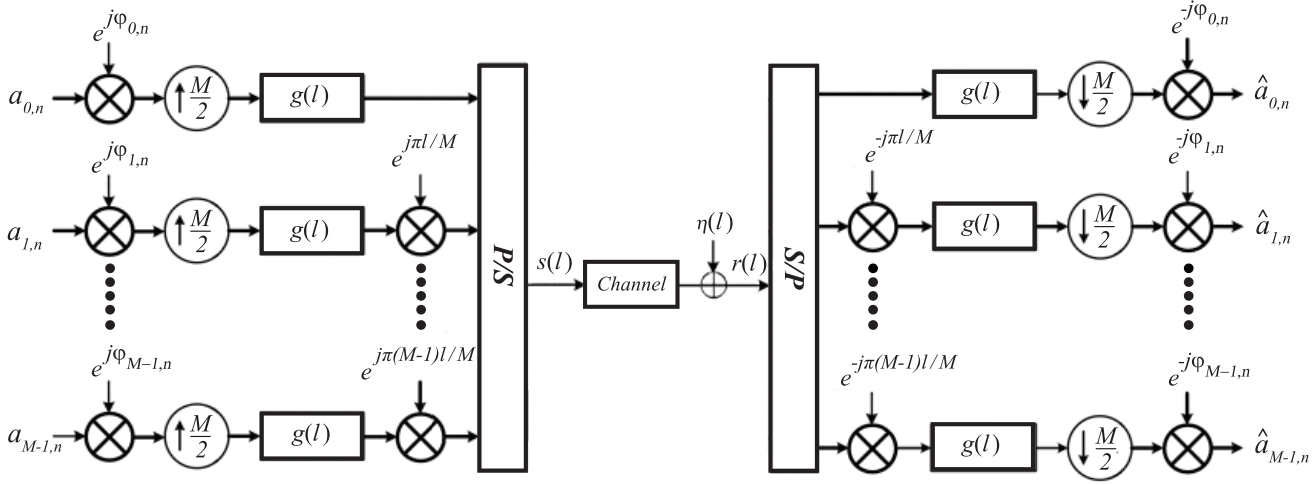

Fig. 1. FBMC-OQAM system model.

II. FBMC-OQAM System Model

A. FBMC-OQAM signal

The discrete-time baseband equivalent of an FBMC-OQAM signal having M sub-carriers is given by [10]

$$s(l) = \sum_{m=0}^{M-1} \sum_{n=-\infty}^{+\infty} a_{m,n} g_{m,n}(l) \quad \forall\, l \in \mathbb{Z}\,, \tag{1}$$

where the pair (m, n) indexes a frequency-time (FT) point. Centred on each FT point (m, n), a real-valued PAM symbol $a_{m,n}$ modulates $g_{m,n}(l)$, which is a phase, frequency and time shifted version of a prototype impulse response $g(l)$, i.e., (assuming M to be even)

$$g_{m,n}(l) \triangleq g\left(l - \frac{nM}{2}\right) e^{j\frac{2\pi}{M}m(l-\frac{L_g-1}{2})} e^{j\varphi_{m,n}} \tag{2}$$

where g is a real linear-phase unit-energy impulse with length $L_g = KM$ samples (K is the time overlapping factor) and $\varphi_{m,n} = (m+n)\frac{\pi}{2} + \varphi_{\mathrm{o}}$ (φ_{o} can be chosen arbitrarily).

A matched filter receiver attempting to detect symbol $a_{p,q}$ has response $g^*_{p,q}$ and its output will contain contributions from each transmitted symbol $a_{m,n}$ given by $a_{m,n}\xi^{p,q}_{m,n}$, where

$$\xi^{p,q}_{m,n} \triangleq \sum_{l=-\infty}^{\infty} g_{m,n}(l) g^*_{p,q}(l)\,. \tag{3}$$

These interference coefficients $\xi^{p,q}_{m,n}$ have symmetry properties in time as well as in frequency, which will be proved in Section III.

The prototype filter used is such that the following real orthogonality condition is satisfied:

$$\Re(\xi^{p,q}_{m,n}) = \Re\left(\sum_{l=-\infty}^{\infty} g_{m,n}(l) g^*_{p,q}(l)\right) = \delta\,[m\text{-}p]\,\delta\,[n\text{-}q] \tag{4}$$

where $\delta\,[.]$ denotes the Kronecker delta function. This condition causes the matched filter output to contain *purely imaginary intrinsic interference*.

B. Reception with time-dispersive channel

For each time instant n, we define a channel vector $\mathbf{h}_n = [h_{0,n}\ h_{1,n}\ \cdots\ h_{M-1,n}]$ whose m-th entry $h_{m,n}$ is the channel gain in sub-carrier m at time instant n. The output of the $(p,q)^{th}$ matched filter is

$$\begin{aligned} y_{p,q} &= \sum_{m,n} h_{m,n}\xi^{p,q}_{m,n} a_{m,n} + w_{p,q} \\ &= h_{p,q}a_{p,q} + \sum_{(m,n)\neq(p,q)} h_{m,n}\xi^{p,q}_{m,n} a_{m,n} + w_{p,q} \end{aligned} \tag{5}$$

where the summation in (5) represents *intrinsic interference* from neighboring symbols and $w_{p,q} = \sum_l \eta(l) g^*_{p,q}(l)$ is colored noise affecting the FT point (p,q), which is a filtered version of the complex AWGN $\eta(l) \sim \mathcal{N}(0, \sigma^2)$ shown in Figure 1.

Typically $\xi^{p,q}_{m,n}$ is zero outside a small neighbouring region about FT grid point (p,q) and if we make the assumption that $h_{m,n} = h_{p,q}$ for this region, then by representing the intrinsic interference affecting $y_{p,q}$ as $h_{p,q}I_{p,q}$, where $I_{p,q} \triangleq \sum_{(m,n)\neq(p,q)} \xi^{p,q}_{m,n} a_{m,n}$, we may rewrite (5) as

$$y_{p,q} = h_{p,q}a_{p,q} + h_{p,q}I_{p,q} + w_{p,q}\,. \tag{6}$$

Given channel estimates $\tilde{h}_{p,q}$, an estimate of the symbol $a_{p,q}$, denoted $\hat{a}_{p,q}$, can be generated by taking the real part of the output from a one-tap equalizer as follows:

$$\hat{a}_{p,q} \triangleq \Re\left(\frac{y_{p,q}}{\tilde{h}_{p,q}}\right) \simeq a_{p,q} + \Re\left(I_{p,q}\right) + \Re\left(\frac{w_{p,q}}{h_{p,q}}\right), \tag{7}$$

where the approximation above is true if $\tilde{h}_{p,q} = h_{p,q}$. These channel estimates could be obtained by various methods such as those described in [8], [11] and [12], all of which require knowledge of $\xi^{p,q}_{m,n}$ and various correlation matrices thus motivating this work.

III. Interference Symmetry Identities

The following theorem provides various symmetry identities for $\xi_{m,n}^{p,q}$ that will be useful in developing autocorrelation matrices in Section IV.

Theorem 1. *For $\delta_p, \delta_q \in \mathbb{Z}$ we have the following properties:*

$$\textit{Conjugate Symmetry:} \quad \xi_{m,n}^{p,q} = \left(\xi_{p,q}^{m,n}\right)^* \tag{8}$$

$$\textit{Frequency Symmetry:} \quad \xi_{p\text{-}\delta_p,n}^{p,q} = (\text{-}1)^{n-q}\left(\xi_{p+\delta_p,n}^{p,q}\right)^* \tag{9}$$

$$\textit{Time Symmetry:} \quad \xi_{m,q\text{-}\delta_q}^{p,q} = (\text{-}1)^{(1+m-p)\delta_q}\xi_{m,q+\delta_q}^{p,q} \tag{10}$$

$$\textit{Frequency Translation:} \quad \xi_{m+\delta_p,n}^{p+\delta_p,q} = \xi_{m,n}^{p,q} \tag{11}$$

$$\textit{Time Translation:} \quad \xi_{m,n+\delta_q}^{p,q+\delta_q} = (\text{-}1)^{(m-p)\delta_q}\xi_{m,n}^{p,q} \tag{12}$$

Proof. Preliminaries:
Rearranging (2) we get

$$g_{m,n}(l) = e^{j(\varphi_{m,n}\text{-}m\frac{L_g\text{-}1}{M}\pi)}g\left(l\text{-}n\frac{M}{2}\right)e^{jm\frac{2\pi}{M}l}$$

where it is now clear that each $g_{m,n}(l)$ is just a time and frequency shifted version of the prototype filter $g(l)$ with a phase rotation. Thus we can now write (3) as:

$$\xi_{m,n}^{p,q} = e^{j\phi(m,n,p,q)}\sum_{l=-\infty}^{\infty} g\left(l\text{-}n\frac{M}{2}\right)g\left(l\text{-}q\frac{M}{2}\right)e^{j(m\text{-}p)\frac{2\pi}{M}l} \tag{13}$$

where $\phi(m,n,p,q) \triangleq \varphi_{m,n}\text{-}\varphi_{p,q}\text{+}(p\text{-}m)\frac{L_g\text{-}1}{M}\pi$.

Proof of (8): Using (13) we have:

$$\begin{aligned}\xi_{m,n}^{p,q} &= e^{j\phi(m,n,p,q)}\sum_{l=-\infty}^{\infty} g\left(l\text{-}n\frac{M}{2}\right)g\left(l\text{-}q\frac{M}{2}\right)e^{j(m\text{-}p)\frac{2\pi}{M}l}\\ &= e^{j\phi(m,n,p,q)}(e^{\text{-}j\phi(p,q,m,n)}\xi_{p,q}^{m,n})^* = (\xi_{p,q}^{m,n})^*\end{aligned}$$

as required. We call this the conjugate symmetry property.

Proof of (9): When receiving the symbol at FT point (p,q) the interference from an FT point having a frequency shift of δ_p is, from (13), given by:

$$\begin{aligned}\xi_{p\text{-}\delta_p,n}^{p,q} &= e^{j\phi(p\text{-}\delta_p,n,p,q)}\sum_{l=-\infty}^{\infty} g\left(l\text{-}n\frac{M}{2}\right)g\left(l\text{-}q\frac{M}{2}\right)e^{\text{-}j\delta_p\frac{2\pi}{M}l}\\ &= e^{j\phi(p\text{-}\delta_p,n,p,q)}\left(e^{\text{-}j\phi(p+\delta_p,n,p,q)}\xi_{p+\delta_p,n}^{p,q}\right)^*\\ &= (\text{-}1)^{n-q}\left(\xi_{p+\delta_p,n}^{p,q}\right)^*\end{aligned}$$

as required. We call this symmetry in the frequency domain.

Proof of (10): When receiving the symbol at FT point (p,q) the interference from an FT point having a time shift of δ_q is, from (13), given by:

$$\begin{aligned}\xi_{m,q\text{-}\delta_q}^{p,q} &= e^{j\phi(m,q\text{-}\delta_q,p,q)}\sum_{l=-\infty}^{\infty} g\left(l\text{-}(q\text{-}\delta_q)\frac{M}{2}\right)g\left(l\text{-}q\frac{M}{2}\right)e^{j(m\text{-}p)\frac{2\pi}{M}l}\\ &= e^{j\phi(m,q\text{-}\delta_q,p,q)}e^{j(m\text{-}p)q\pi}\sum_{u=-\infty}^{\infty} g\left(u\text{+}\delta_q\frac{M}{2}\right)g(u)\,e^{j(m\text{-}p)\frac{2\pi}{M}u}\end{aligned}$$

Similarly we have:

$$\begin{aligned}\xi_{m,q+\delta_q}^{p,q} &= e^{j\phi(m,q+\delta_q,p,q)}\sum_{l=-\infty}^{\infty} g\left(l\text{-}(q\text{+}\delta_q)\frac{M}{2}\right)g\left(l\text{-}q\frac{M}{2}\right)e^{j(m\text{-}p)\frac{2\pi}{M}l}\\ &= e^{j\phi(m,q+\delta_q,p,q)}e^{j(m\text{-}p)(q+\delta_q)\pi}\sum_{u=-\infty}^{\infty} g(u)g\left(u\text{+}\delta_q\frac{M}{2}\right)e^{j(m\text{-}p)\frac{2\pi}{M}u}\end{aligned}$$

The summation in the two previous results are the same thus:

$$\begin{aligned}&\xi_{m,q\text{-}\delta_q}^{p,q} =\\ &e^{j\phi(m,q\text{-}\delta_q,p,q)}e^{j(m\text{-}p)q\pi}e^{\text{-}j\phi(m,q+\delta_q,p,q)}e^{\text{-}j(m\text{-}p)(q+\delta_q)\pi}\xi_{m,q+\delta_q}^{p,q}\\ &\quad = e^{\text{-}j\delta_q\pi}e^{\text{-}j(m\text{-}p)\delta_q\pi}\xi_{m,q+\delta_q}^{p,q} = (\text{-}1)^{(1+m-p)\delta_q}\xi_{m,q+\delta_q}^{p,q}\end{aligned}$$

as required. We call this symmetry in the time domain.

Proof of (11): Using (13) we can calculate:

$$\begin{aligned}&\xi_{m+\delta_p,n}^{p+\delta_p,q} =\\ &e^{j\phi(m+\delta_p,n,p+\delta_p,q)}\sum_{l=-\infty}^{\infty} g\left(l\text{-}n\tfrac{M}{2}\right)g\left(l\text{-}q\tfrac{M}{2}\right)e^{j((m+\delta_p)\text{-}(p+\delta_p))\frac{2\pi}{M}l}\end{aligned}$$

Since, $\phi(m\text{+}\delta_p,n,p\text{+}\delta_p,q) = \phi(m,n,p,q)$. Thus,

$$\xi_{m+\delta_p,n}^{p+\delta_p,q} = e^{j\phi(m,n,p,q)}\sum_{l=-\infty}^{\infty} g\left(l\text{-}n\tfrac{M}{2}\right)g\left(l\text{-}q\tfrac{M}{2}\right)e^{j(m\text{-}p)\frac{2\pi}{M}l} = \xi_{m,n}^{p,q}$$

as required. We call this frequency translation property.

Proof of (12): Using (13) we can calculate:

$$\begin{aligned}&\xi_{m,n+\delta_q}^{p,q+\delta_q} =\\ &e^{j\phi(m,n+\delta_q,p,q+\delta_q)}\sum_{l=-\infty}^{\infty} g\left(l\text{-}(n\text{+}\delta_q)\tfrac{M}{2}\right)g\left(l\text{-}(q\text{+}\delta_q)\tfrac{M}{2}\right)e^{j(m\text{-}p)\frac{2\pi}{M}l}\end{aligned}$$

Since, $\phi(m,n\text{+}\delta_q,p,q\text{+}\delta_q) = \phi(m,n,p,q)$ and applying change of variable as $(u - q\frac{M}{2}) = (l - (q+\delta_q)\frac{M}{2})$. Thus obtaining,

$$\begin{aligned}&\xi_{m,n+\delta_q}^{p,q+\delta_q} =\\ &e^{\text{-}j(m\text{-}p)(\delta_p)\pi}e^{j\phi(m,n,p,q)}\sum_{u=-\infty}^{\infty} g\left(u\text{-}q\tfrac{M}{2}\right)g\left(u\text{-}n\tfrac{M}{2}\right)e^{j(m\text{-}p)\frac{2\pi}{M}l}\\ &\qquad = (\text{-}1)^{(m-p)\delta_q}\xi_{m,n}^{p,q}\end{aligned}$$

as required. We call this the time translation property.
This completes the proofs. □

IV. Application: Autocorrelation matrices

The symmetric nature of the interference coefficients has been used to design a number of receiver algorithms. These symmetry properties allow for ease of calculation of the interference power on a particular symbol in the frequency-time grid which can, in turn, underpin schemes for interference cancellation [11] and interference approximation [12] to improve the channel estimates, as well as calculation of the autocorrelation matrices for the relevant noise and interference

terms. Note that previous works such as [11], [12] considered only the frequency symmetry in immediate neighborhood (i.e., $|\delta_p| = 1$) to design their schemes for channel estimations. In contrast, the result expressed in Theorem 1 represents a set of general symmetry conditions which are valid for all points in the FT grid. In this section, we describe the applications of these symmetry conditions.

A. Noise Autocorrelation Matrix

In FBMC-OQAM, the filtered noise is correlated among sub-carriers. The filtered noise at FT point (p, q) is $w_{p,q} = \sum_l \eta(l) g^*_{p,q}$, which can be written as

$$w_{p,q} = \sum_l \eta(l) g(l - \frac{qM}{2}) e^{-j\frac{2\pi}{M}p(l-\frac{L_g-1}{2})} e^{-j\varphi_{p,q}} . \quad (14)$$

Since linear filtering of a zero-mean Gaussian random process yields another zero-mean Gaussian process, thus also $E[w_{p,q}] = 0$. Considering the prototype filter g be unit energy, the variance of $w_{p,q}$ is given by

$$\sigma_w^2 = E[w_{p,q} w^*_{p,q}] = \sigma^2 \sum_l g^2(l - \frac{qM}{2}) = \sigma^2 \quad (15)$$

Next consider two FT points (p_1, q_1) and (p_2, q_2). The filtered noise contributions at these points are w_{p_1,q_1} and w_{p_2,q_2} respectively, and their covariance is given by $\mathrm{Cov}[w_{p_1,q_1}, w_{p_2,q_2}] = E[w_{p_1,q_1} w^*_{p_2,q_2}]$, i.e.,

$$\mathrm{Cov}[w_{p_1,q_1}, w_{p_2,q_2}] = \sigma^2 \sum_l g^*_{p_1,q_1} g_{p_2,q_2} = \sigma^2 \xi^{p_2,q_2}_{p_1,q_1} . \quad (16)$$

Using (16) and considering M neighboring sub-carriers at an arbitrary time instant n, we can write the noise covariance matrix of size $M \times M$ for $[w_{0,n}\ w_{1,n}\ \cdots\ w_{M-1,n}]$ as

$$\mathbf{B}^{(n)} = \sigma^2 \begin{bmatrix} 1 & \xi^{1,n}_{0,n} & \xi^{2,n}_{0,n} & \cdots & \xi^{M-1,n}_{0,n} \\ \xi^{0,n}_{1,n} & 1 & \xi^{2,n}_{1,n} & \cdots & \xi^{M-1,n}_{1,n} \\ \xi^{0,n}_{2,n} & \xi^{1,n}_{2,n} & 1 & \cdots & \xi^{M-1,n}_{2,n} \\ \vdots & \vdots & \vdots & \ddots & \vdots \\ \xi^{0,n}_{M-1,n} & \xi^{1,n}_{M-1,n} & \xi^{2,n}_{M-1,n} & \cdots & 1 \end{bmatrix} \quad (17)$$

Considering (11), in the matrix $\mathbf{B}^{(n)}$ the interference coefficients in each diagonal are equal, making the noise covariance matrix a Toeplitz matrix. Also, the conjugate symmetry property of $\xi^{p,q}_{m,n}$ given by (8) implies that the matrix $\mathbf{B}^{(n)}$ is conjugate symmetric. Finally, from (4), $\xi^{p,q}_{m,n}$ is purely imaginary for all $(p, q) \neq (m, n)$, making $\Re(\mathbf{B}^{(n)}) = \mathbf{I}$.

Letting $\mathbf{B}^{(n)}_{x,y}$ as the $(x, y)^{th}$ element of $\mathbf{B}^{(n)}$ and using (12) we can obtain,

$$\mathbf{B}^{(n)}_{x,y} = (-1)^{(p-m)n} \mathbf{B}^{(0)}_{x,y} \quad (18)$$

Using (18), we can find that there are in fact only two unique $\mathbf{B}^{(n)}$ matrices exist i.e.,

$$\mathbf{B}^{(n)} = \begin{cases} \mathbf{B}^{(0)} & \text{for } n \text{ even} \\ \mathbf{B}^{(1)} & \text{for } n \text{ odd} \end{cases} \quad (19)$$

It could also be seen from (18), that $\mathbf{B}^{(1)}$ can be easily obtained from $\mathbf{B}^{(0)}$ by multiplying each of its element with $(-1)^{x-y}$.

B. Interference Autocorrelation Matrix

Some authors (e.g. [13]), have need to compute the autocorrelation matrix of $I_{p,q}$ under the assumption that $h_{m,n} = 1$ for all m and n. Thus, from the definition of interference in FBMC-OQAM we get,

$$I_{p,q}|_{h_{m,n}=1} = \sum_{(m,n)\neq(p,q)} a_{m,n} \xi^{p,q}_{m,n} \quad (20)$$

The autocorrelation matrix $\mathbf{C}_q$, of the above considering M neighboring sub-carrier at a time instant q can be written as

$$[\mathbf{C}_q]_{i,j} \triangleq E\left[I_{i,q}, I^*_{j,q}\right]\big|_{h_{m,n}=1} = \sigma_a^2 \sum_{\substack{(m,n)\neq(i,q) \\ (m,n)\neq(j,q)}} \xi^{i,q}_{m,n} (\xi^{j,q}_{m,n})^* \quad (21)$$

where σ_a^2 is the variance of independent data symbols $a_{m,n}$. As with all autocorrelation matrices $\mathbf{C}_q$ exhibits conjugate symmetry, but it also has the following properties. The i^{th} diagonal entry is given by:

$$[\mathbf{C}_q]_{i,i} = \sigma_a^2 \sum_{(m,n)\neq(i,q)} |\xi^{i,q}_{m,n}|^2 \quad (22)$$

which by using (11) can be shown to be a constant for all i. Similarly for the other (non-diagonal) elements it can be shown that:

$$[\mathbf{C}_q]_{i+\delta_p, j+\delta_p} = [\mathbf{C}_q]_{i,j} \quad (23)$$

i.e. similar to (17), $\mathbf{C}_q$ is also a Toeplitz matrix.

V. Illustrative examples

In this section, we provide some examples which illustrate the symmetry properties described by Theorem 1. The calculations are performed using four different prototype filters of whose the time domain expressions and parameters are given in Table I. A time domain comparison of the pulse shape for these prototype filters is given in Fig. 2; Fig. 3 presents the corresponding comparison in the frequency domain. The interference coefficients $\xi^{p,q}_{m,n}$ is presented in tabular form for various prototype filters mentioned in Section I as: Table II for the PHYDYAS prototype filter; Table III for the Hermite polynomial based prototype filter; Table IV for the RRC prototype filter; and Table V for the half cosine prototype filter. For ease of presentation of these results, we have approximated values $|\xi^{m,n}_{p,q}|$ smaller that 0.0002 to zero.

From Tables II and V it can be seen that the PHYDYAS and half cosine prototype filters have better interference confinement in frequency than in time. For the Hermite polynomial based filter, the interference confinement is better in time, whereas for the RRC filter with $\beta = 0.5$ the confinement is poor in both frequency and time axis. The frequency and time symmetry of interference coefficients is also indicated in Tables II, III, IV and V; it can be seen that the symmetry conditions always hold irrespective of the prototype filter applied.

TABLE I
TIME DOMAIN EXPRESSIONS OF THE PROTOTYPE FILTERS CONSIDERED IN FBMC-OQAM SYSTEM IMPLEMENTATION

Prototype Filter	Analytical Expression	Parameters
PHYDYAS	$g(l) = 1 + 2\sum_{k=1}^{K-1}(-1)^k H_k^2 cos(2\pi \frac{kl}{KT})$	$K = 4$ $H_0 = 1$ $H_1 = 0.97195983$ $H_2 = 0.70710681$ $H_3 = 0.23514695$
Hermite	$g(l) = \sum_{k=0}^{K} z_{4k}\Phi_{4k}(l)$ $\Phi_{4k}(l) = H_n(\sqrt{2\pi}l)e^{-\pi l^2}$ $H_n(l) = (-1)^n e^{l^2}\frac{d^n}{dl^n}e^{-l^2}$	$K = 4$ $z_0 = 1.1850899$ $z_4 = 1.9324881$ x $10^{-3} z_0$ $z_8 = 7.3110588$ x $10^{-6} z_0$ $z_{12} = 3.1542096$ x $10^{-9} z_0$ $z_{16} = 9.6634138$ x $10^{-13} z_0$
Root Raised Cosine (RRC)	$g(l) = \begin{cases} \frac{1}{T}\left(1+\beta(\frac{4}{\pi}-1)\right), & l=0 \\ \frac{\beta}{T\sqrt{2}}\left[\left(1+\frac{2}{\pi}\right)\sin\left(\frac{\pi}{4\beta}\right)+\left(1-\frac{2}{\pi}\right)\cos\left(\frac{\pi}{4\beta}\right)\right], & l=\pm\frac{T}{4\beta} \\ \frac{1}{T}\frac{\sin\left[\pi\frac{l}{T}(1-\beta)\right]+4\beta\frac{l}{T}\cos\left[\pi\frac{l}{T}(1+\beta)\right]}{\pi\frac{l}{T}\left[1-\left(4\beta\frac{l}{T}\right)^2\right]}, & \text{otherwise} \end{cases}$	$\beta = 0.5$
Half Cosine	$g(l) = \begin{cases} \frac{1}{T}\left(1+\beta(\frac{4}{\pi}-1)\right), & l=0 \\ \frac{\beta}{T\sqrt{2}}\left[\left(1+\frac{2}{\pi}\right)\sin\left(\frac{\pi}{4\beta}\right)+\left(1-\frac{2}{\pi}\right)\cos\left(\frac{\pi}{4\beta}\right)\right], & l=\pm\frac{T}{4\beta} \\ \frac{1}{T}\frac{\sin\left[\pi\frac{l}{T}(1-\beta)\right]+4\beta\frac{l}{T}\cos\left[\pi\frac{l}{T}(1+\beta)\right]}{\pi\frac{l}{T}\left[1-\left(4\beta\frac{l}{T}\right)^2\right]}, & \text{otherwise} \end{cases}$	$\beta = 1$

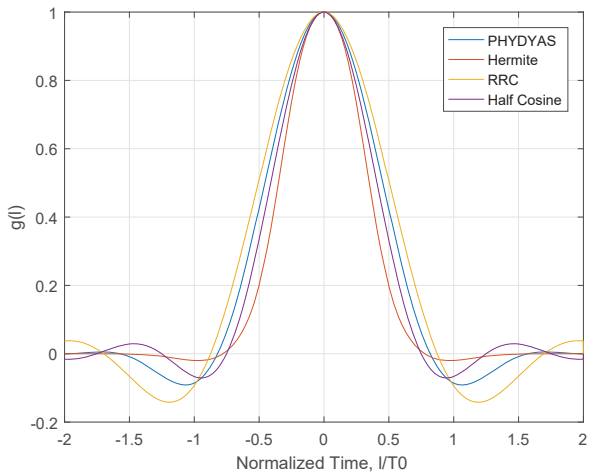

Fig. 2. FBMC-OQAM Prototype Filters in the Time Domain, where T0 is the symbol period.

TABLE II
$\xi_{m,n}^{p,q}$ TABLE FOR EVEN p USING PHYDYAS FILTER [$K = 4$]. THE ENTRIES MARKED WITH † ARE NEGATED FOR p ODD.

	q-3	q-2	q-1	n=q	q+1	q+2	q+3
p+3	0	0	0	0	0	0	0
p+2	j0.0006†	0	0	0	0	0	-j0.0006†
p+1	-j0.0429†	-j0.125	-j0.2058†	-j0.2393	-j0.2058†	-j0.125	-j0.0429†
m=p	j0.0668†	0	j0.5644†	1	-j0.5644†	0	-j0.0668†
p-1	-j0.0429†	j0.125	-j0.2058†	j0.2393	-j0.2058†	j0.125	-j0.0429†
p-2	j0.0006†	0	0	0	0	0	-j0.0006†
p+4	0	0	0	0	0	0	0

TABLE III
$\xi_{m,n}^{p,q}$ TABLE FOR EVEN p USING HERMITE FILTER [$K = 4$]. THE ENTRIES MARKED WITH † ARE NEGATED FOR p ODD.

	q-3	q-2	q-1	n=q	q+1	q+2	q+3
p+3	0	-j0.0003	-j0.0054†	j0.0098	-j0.0054†	-j0.0003	0
p+2	j0.0003†	0	j0.0369†	0	-j0.0369†	0	-j0.0003†
p+1	-j0.0054†	j0.0369	-j0.2393†	-j0.4357	-j0.2393†	j0.0369	-j0.0054†
m=p	j0.0098†	0	j0.4357†	1	-j0.4357†	0	-j0.0098†
p-1	-j0.0054†	-j0.0369	-j0.2393†	j0.4357	-j0.2393†	-j0.0369	-j0.0054†
p-2	j0.0003†	0	j0.0369†	0	-j0.0369†	0	-j0.0003†
p+4	0	j0.0003	-j0.0054†	-j0.0098	-j0.0054†	j0.0003	0

VI. CONCLUSION

FBMC-OQAM is orthogonal in the real domain, but some residual interference always exists which is imaginary in nature. This interference possesses a symmetric nature which allows for ease of design of receiver algorithms for FBMC-OQAM systems. In this work we have proved a set of general symmetry properties satisfied by FBMC-OQAM's interference, which have been shown to hold regardless of the prototype filter employed.

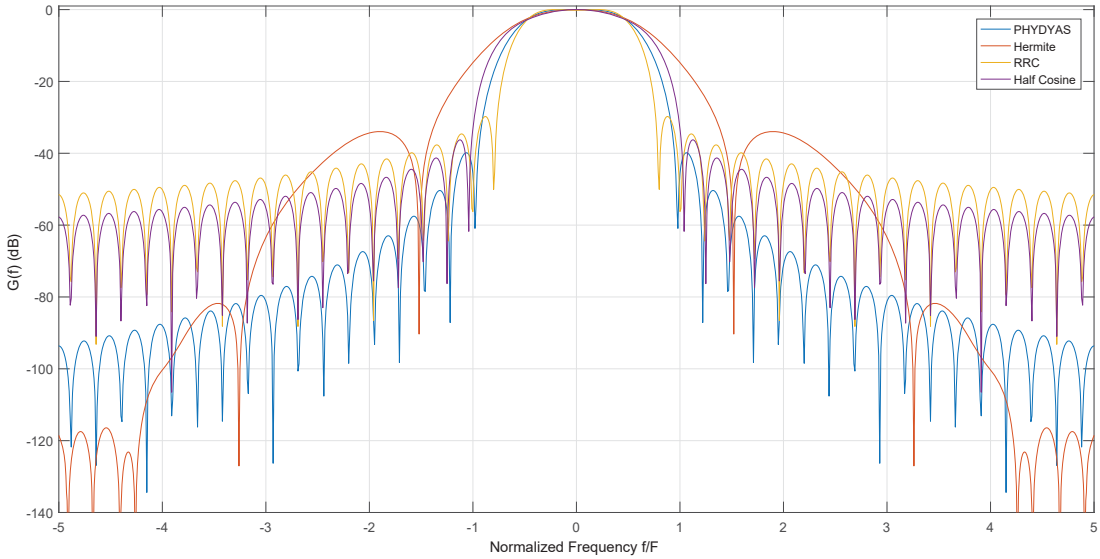

Fig. 3. FBMC-OQAM Prototype Filters in Frequency Domain, where F is the sub-carrier spacing.

TABLE IV
$\xi_{m,n}^{p,q}$ TABLE FOR EVEN p USING RRC FILTER [ROLLOFF $\beta = 0.50$]. THE ENTRIES MARKED WITH † ARE NEGATED FOR p ODD.

	q-3	q-2	q-1	n=q	q+1	q+2	q+3
p+3	-j0.0027†	0	-j0.0003†	0	-j0.0003†	0	-j0.0027†
p+2	j0.0020†	0	j0.0004†	0	-j0.0004†	0	-j0.0020†
p+1	-j0.0920†	-j0.1233	-j0.1503†	-j0.1591	-j0.1503†	-j0.1233	-j0.0920†
m=p	j0.1290†	0	j0.6021†	1	-j0.6021†	0	-j0.1290†
p-1	-j0.0920†	j0.1233	-j0.1503†	j0.1591	-j0.1503†	j0.1233	-j0.0920†
p-2	j0.0020†	0	j0.0004†	0	-j0.0004†	0	-j0.0020†
p+4	-j0.0027†	0	-j0.0003†	0	-j0.0003†	0	-j0.0027†

TABLE V
$\xi_{m,n}^{p,q}$ TABLE FOR EVEN p USING HALF COSINE FILTER. THE ENTRIES MARKED WITH † ARE NEGATED FOR p ODD.

	q-3	q-2	q-1	n=q	q+1	q+2	q+3
p+3	-j0.0009†	0	0	0	0	0	-j0.0009†
p+2	j0.0013†	0	0	0	0	0	-j0.0013†
p+1	-j0.0006†	-j0.1063	-j0.2501†	-j0.3184	-j0.2501†	-j0.1063	-j0.0006†
m=p	j0.0024†	0	j0.5001†	1	-j0.5001†	0	-j0.0024†
p-1	-j0.0006†	j0.1063	-j0.2501†	j0.3184	-j0.2501†	j0.1063	-j0.0006†
p-2	j0.0013†	0	0	0	0	0	-j0.0013†
p+4	-j0.0009†	0	0	0	0	0	-j0.0009†

REFERENCES

[1] R. v. Nee and R. Prasad, *OFDM for wireless multimedia communications*. Artech House, Inc., 2000.

[2] J. G. Andrews, S. Buzzi, W. Choi, S. V. Hanly, A. Lozano, A. C. Soong, and J. C. Zhang, "What will 5g be?" *IEEE Journal on selected areas in communications*, vol. 32, no. 6, pp. 1065–1082, 2014.

[3] B. Farhang-Boroujeny, "OFDM versus filter bank multicarrier," *IEEE signal processing magazine*, vol. 28, no. 3, pp. 92–112, 2011.

[4] M. G. Bellanger, "Specification and design of a prototype filter for filter bank based multicarrier transmission," in *Acoustics, Speech, and Signal Processing, 2001. Proceedings.(ICASSP'01). 2001 IEEE International Conference on*, vol. 4. IEEE, 2001, pp. 2417–2420.

[5] R. Haas and J.-C. Belfiore, "A time-frequency well-localized pulse for multiple carrier transmission," *Wireless personal communications*, vol. 5, no. 1, pp. 1–18, 1997.

[6] B. Farhang-Boroujeny, *Signal processing techniques for software radios*. Lulu publishing house Raleigh, 2008.

[7] J. Du and S. Signell, "Classic OFDM systems and pulse shaping OFDM/OQAM systems," 2007.

[8] E. Kofidis, D. Katselis, A. Rontogiannis, and S. Theodoridis, "Preamble-based channel estimation in OFDM/OQAM systems: A review," *Signal Processing*, vol. 93, no. 7, pp. 2038–2054, 2013.

[9] E. Kofidis and D. Katselis, "Improved interference approximation method for preamble-based channel estimation in FBMC/OQAM," in *Signal Processing Conference, 2011 19th European*. IEEE, 2011, pp. 1603–1607.

[10] M. Bellanger, D. Le Ruyet, D. Roviras, M. Terré, J. Nossek, L. Baltar, Q. Bai, D. Waldhauser, M. Renfors, T. Ihalainen *et al.*, "FBMC physical layer: a primer," *PHYDYAS, January*, vol. 25, no. 4, pp. 7–10, 2010.

[11] S. Kang and K. Chang, "A novel channel estimation scheme for OFDM/OQAM-IOTA system," *ETRI journal*, vol. 29, no. 4, pp. 430–436, 2007.

[12] D. Lacroix and J.-P. Javaudin, "A new channel estimation method for OFDM/OQAM," in *7th International OFDM-Workshop*, 2002.

[13] V. K. Singh, M. F. Flanagan, and B. Cardiff, "Generalized least squares based channel estimation for high data rate FBMC-OQAM," in *2018 25th International Conference on Telecommunications (ICT) (ICT 2018)*, Saint Malo, France, Jun. 2018.